# CERAMIC TILES WITH VERY LOW DENSITY DEVELOPED BY RECYCLING GLAZE WASTE

**Giovani Nesi, Adriano Michael Bernardin**

Ceramic Materials Group, UNESC, Criciúma, Santa Catarina, Brazil

## ABSTRACT

The ceramic industry generates large quantities of waste, which is usually deposited in landfills. On the other hand, waste recovery and recycling are very attractive from the standpoint of economic and environmental solutions, this being a reality today in ceramic industries. Therefore, this paper addresses the reuse of glaze waste derived from an effluent treatment plant in the development of ceramic tiles for façades with low density. The glaze waste was characterized (XRF) and silicon carbide (0.05 wt%) was added to the glaze waste as bubbling agent and CMC (10 wt%) was added to the mixture as a binder. The mixture was granulated (7 wt% water) and compacted by double loading using a standard stoneware body as substrate according to a 2k full factorial experimental design (DoE). The amount of stoneware body in relation to the waste in the double loading and the compaction pressure were the factors. After drying, the compacts were fired in a roller kiln to 1180°C in 44 min cycle. The fired samples were characterized for the determination of the thermal expansion, modulus of flexural strength, water absorption and apparent density. The results clearly showed the effect of the double loading on these properties, and it was possible to obtain tiles with very low density (0.8 g/cm$^3$) and a cellular structure.

## 1. INTRODUCTION

In the ceramic industry the reuse and recycling of waste is very effective because it reduces waste formation as well as the excessive consumption of natural resources. Also, waste from one company can be considered raw material for another. Recycling is the reintroduction of final products, by-products and waste in a new production and consumption cycle. The recycling of wastes that have economic value is one of the most attractive ways to solve problems related to waste treatment and disposal.

The scrap or waste derived from ceramic processing generally consists of defective tiles, products that present some type of defect and therefore are declassified and disposed of in landfills. Liquid effluents contain inorganic insoluble substances. Ceramic pigments contain Al, Co, Zr, Se, Cr, Zn, Ni, Ca and Sn oxides. Glazes contain $B_2O_3$, ZnO and PbO. Synthetic resins contain organic composites. Ceramic inks contain Pb, Ca, Se, Al, Fe, Cr and Mn. Also, there are fine particulates in suspension (clays, glaze rests, silicates). The solid wastes issue includes aspects relating to their origin and production, as well as concepts of inexhaustibility and the consequences of ground, air and water environmental degradation.

Waste formation and accumulation are increasing and the treatment techniques often become economically impracticable. The technological improvement of waste treatment depends on recycling infrastructure and consumption volume of manufactured products. Waste is generally considered an inevitable by-product of mass production. But nowadays the industrial sector has developed a recycling awareness, as the consumer market has demanded this attitude of them.

In order to define an adequate solid waste management program, waste classification becomes necessary. Industrial solid wastes can be classified as dangerous and non-dangerous. This differentiation is important and necessary because the management program for each type of waste is very different, taking into consideration technology and costs.

The ceramic industry of Santa Catarina state is the second major Brazilian ceramic complex. The ceramic tile industry of the Criciúma region does not have any governmental recycling program for solid wastes. The industrial solid wastes are dumped directly at landfills. Ceramic companies dispose of glazing and polishing process waste without any criterion. Glazing waste consists of rests from the glaze application processes, which are recovered, stored and filtered to eliminate waste water. The product of the filtration process is landfilled. Polishing waste is handled in the same way.

An alternative to the dumping of the solid wastes generated by the ceramic industry (glazing and polishing waste) is the reuse of this waste as raw materials for new products, like cellular ceramics. These products are useful in the construction industry as filling materials, substituting expanded polymers or even substituting wood and paper. In addition, these products have excellent thermal and acoustic insulation characteristics.

Therefore, the main objective of this work was the development of low density ceramic tiles using glazing process waste as raw materials.

## 2. MATERIALS AND METHODS

This work was developed in the laboratory facilities of Novagrés Ceramics (Urussanga, Santa Catarina, Brazil) using industrial glazing waste. A 50 kg sample was collected, homogenized and dried in laboratory oven at 110 °C for 24 hours. The chemical analysis of the glaze waste was determined by X-ray fluorescence (Philips mod. PW2400, the sample was fused using lithium tetraborate for analysis). After drying, the glaze waste was disaggregated in a laboratory mill (500 mL) using high-alumina grinding elements (70% small and 30% medium-sized balls, by volume) for 30 min and sieved at 50 mesh. After sieving, 0.05 wt% silicon carbide was added to the glaze waste and mixed manually. SiC was used as foaming agent to reduce the density of the tiles and to form the cellular ceramics.

The cellular ceramics (or ceramic foams) developed in this work were made by the bubble formation foaming technique using a foaming agent: the silicon carbide added to the glaze waste oxidizes above 1000°C in the presence of oxygen. Its oxidation results in silica and carbon dioxide according to: $SiC+2O_2 = SiO_2+CO_2$ (reduced formula). Therefore, the mixture of a vitreous material that melts at the same temperature as SiC oxidation can result in a cellular ceramic material because of gas evolution during firing.

After mixing, an aqueous solution formed by 10 wt% carboxymethylcellulose (CMC) and 90 wt% water was used as binder. 10 wt% of the binder solution was added to the mix (SiC + glaze waste) in order to improve the compaction during pressing. The mixture with binder was sieved (50 mesh ASTM) for granulation and homogenized for 24 hours, forming the glaze + SiC pressing powder.

The glaze + SiC pressing powder was compacted in a double-loading sequence in a laboratory hydraulic press according to a statistical experimental design. The double-loading sequence consisted of a first layer formed by a standard stoneware powder as substrate and a second layer formed by the glaze + SiC pressing powder. First, the standard spray-dried stoneware powder was filled in the press moulds in layers of 1/3, ½ and 2/3 of the mould height. In sequence, the glaze + SiC pressing powder was filled over the stoneware powder in layers of 2/3, ½ and 1/3 of the mould height. After loading, the double layer powder was pressed with pressing loads of 30, 45 and 60 MPa, resulting in specimens with 100 mm length, 30 mm width and 5 mm thickness. Therefore, the factors of the experimental design were the fraction of double-loading and compaction pressure. The central points were the ½ layer (50% stoneware and 50% waste, by height) and the 45 MPa pressing load.

Six samples of each test were pressed and dried in laboratory oven at 110°C for 2 hours to constant weight. The specimens were fired in an industrial roller kiln for 44 min at a maximum temperature of 1180°C with 3.4 minutes of holding time at the maximum temperature.

After firing, the specimens were subjected to physical testing according to the apparent density, firing expansion, modulus of rupture and water absorption testing procedures (EN 10545 standards). The apparent density of the green and fired samples was measured by mercury immersion (Archimedes) technique. The expansion after firing was determined by measuring the dimensions of the samples before and after firing.

The modulus of rupture was determined by the three-point bending test using a load application rate of 1 MPa/s until failure (breaking) of the samples. The water absorption was determined by immersing the samples for 2 hours in boiling water. All tests were carried out according the EN 10545 standard procedures. Finally, 2 cm x 2 cm samples were prepared for microstructural analysis by scanning electron microscopy (SEM). All results were analysed by analysis of variance (ANOVA) and contour lines or averages were graphically obtained from the response surfaces for each test

## 3. RESULTS AND DISCUSSION

Table 1 shows the chemical composition of the glazing waste. Table 2 shows the $2^k$ experimental design with four blocks and two central points and the results for bulk density for green and fired samples, water absorption, firing expansion and modulus of rupture for bending strength.

| Oxide (wt %) | $SiO_2$ | $Al_2O_3$ | MgO | $K_2O$ | $Na_2O$ | $ZrO_2$ | CaO | $Fe_2O_3$ | $TiO_2$ | ppc |
|---|---|---|---|---|---|---|---|---|---|---|
| Glazing waste | 63.1 | 16.7 | 6.1 | 2.3 | 2.0 | 1.7 | 1.3 | 0.6 | 0.3 | 5.7 |

*Table 1. Chemical analysis of the glazing waste (XRF).*

The chemical composition of the glazing waste displays the composition of a typical mixture of frits widely used in the ceramic tile industry. Silica and alumina are the major components. Alkali and alkaline earth oxides are fluxing materials. Iron and titanium oxides are contaminants and the loss on ignition is related with organic matter, as the waste was obtained from an effluent treatment station. The presence of zirconia, common in white frits, is worth noting. It was not possible to determine the presence of lithium or boron because those components are not identified by XRF.

| Run | DL | P (MPa) | $d_g$ (g/cm³) | $d_f$ (g/cm³) | WA (%) | FE (%) | MRB (MPa) |
|---|---|---|---|---|---|---|---|
| 1 | 0.33 | 30 | 1.97 | 0.85 | 2.15 | 5.7 | 5.63 |
| 2 | 0.66 | 30 | 1.65 | 1.17 | 3.33 | 2.2 | 7.43 |
| 3 | 0.33 | 60 | 2 | 0.86 | 2.16 | 7.14 | 6.67 |
| 4 | 0.66 | 60 | 1.6 | 1.16 | 3.03 | 1.98 | 9.16 |
| 5 | 0.33 | 30 | 1.98 | 0.78 | 2.13 | 6.67 | 6.2 |
| 6 | 0.66 | 30 | 1.63 | 1.13 | 3.18 | 2.48 | 7.8 |
| 7 | 0.33 | 60 | 1.99 | 0.85 | 3.3 | 6.34 | 6.34 |
| 8 | 0.66 | 60 | 1.62 | 1.13 | 2.94 | 2.45 | 9.68 |
| 9 (C) | 0.50 | 45 | 1.61 | 1.13 | 2.84 | 3.79 | 8.94 |
| 10 | 0.66 | 60 | 1.61 | 1.14 | 2.4 | 1.91 | 8.71 |
| 11 | 0.33 | 60 | 1.98 | 0.84 | 2.26 | 7.55 | 7.02 |

| | | | | | | | |
|---|---|---|---|---|---|---|---|
| 12 | 0.66 | 30 | 1.62 | 1.16 | 3.33 | 2.26 | 7.66 |
| 13 | 0.33 | 30 | 1.97 | 0.83 | 2.16 | 6.66 | 5.52 |
| 14 | 0.66 | 60 | 1.59 | 1.13 | 3.09 | 1.97 | 8.97 |
| 15 | 0.33 | 60 | 1.99 | 0.84 | 2.32 | 7.2 | 6.83 |
| 16 | 0.66 | 30 | 1.61 | 1.1 | 3.15 | 2.66 | 7.17 |
| 17 | 0.33 | 30 | 1.97 | 0.85 | 2.17 | 5.88 | 5.62 |
| 18 (C) | 0.50 | 45 | 1.6 | 1.02 | 2.81 | 3.7 | 8.91 |

*Table 2. 2k experimental design and test results.*

Where: DL is double-loading, P is pressure, dg is green density, df is firing density, WA is water absorption, FE is firing expansion, and MRB is the modulus of rupture in bending

From the results shown in Table 2, the analysis of variance for green density was calculated, Table 3. For the analysis of the most influential factor on density (or double-loading pressing force), initially the factor F (Fisher) must be checked. F shows the largest source of variability, i.e. which model is the most significant for all tests performed in this work. $F_{experimental}$ must be greater than $F_{tabulated}$ for the hypothesis ($H_0$) of the variability factor be true, that is, the higher the significance of the tested model. The analysis of variance shows that the most statistically significant factor, given by the F test, is only the double-loading, with 100% reliability of the results given by the p test. The other factors are not statistically significant, because they showed a value for the $F_{experimental}$ below the tabulated value. The data from the analysis of variance results for the green density were plotted as a function of the average effect of double-loading, Figure 1.

| Factor | SS | dF | MS | F | p |
|---|---|---|---|---|---|
| Doble carga (%) | 0.5329 | 1 | 0.5329 | 109.0 | 0.000 |
| Presión (MPa) | 0.000025 | 1 | 0.000025 | 0.0051 | 0.944 |
| Doble carga × Presión | 0.001600 | 1 | 0.001600 | 0.3273 | 0.576 |
| Error | 0.06844 | 14 | 0.004888 | | |
| SS total | 0.6030 | 17 | | | |

*Table 3. Analysis of variance for the green density.*

Where: SS are the sum of squares; dF degrees of freedom (the difference between the total number of experiments and the number of independent experiments); MS are the mean squares and F and p are reliability tests.

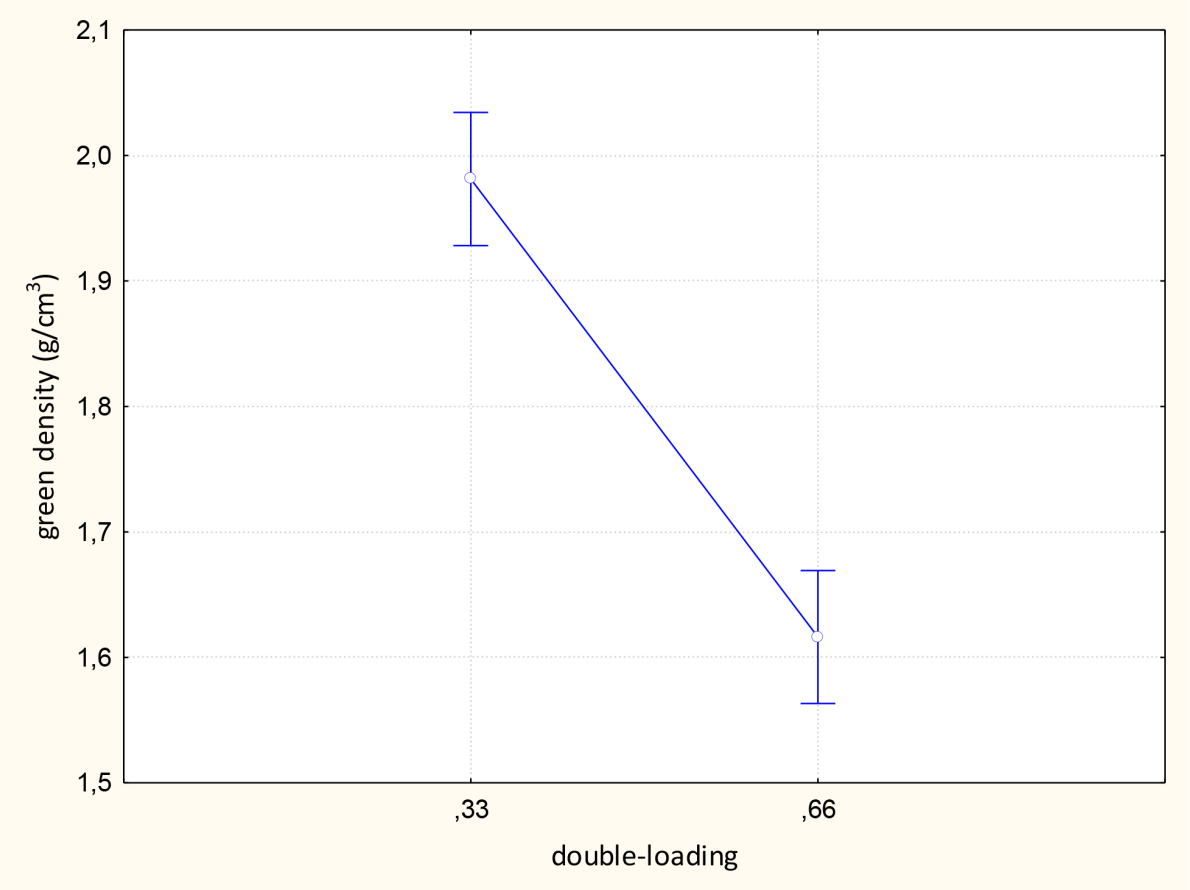


*Figure 1. Averages for green density as a function of double-loading.*

The effect of the double-loading on the green density is evident: the highest values of green density (~2 g/cm³) occur for double-loading with one-third layer of stoneware. As the glazing waste was mixed with a binder (CMC), a major fraction (layer) of waste during compaction (lower fraction of stoneware) results in higher green density due to the higher plasticity of the glazing waste formulated with binder. The fit of the observed results is $R^2$=0.89.

Table 4 shows the analysis of variance for the apparent density after firing. Analysis of variance shows that the most statistically significant factor is again only the double-loading, 100% reliability of the results. The other factors are not statistically significant. The data from the analysis of variance results for bulk density after firing were plotted as a function of the average effect of double-loading, Figure 2.

| Factor | SS | dF | MS | F | p |
|---|---|---|---|---|---|
| Double-loading (%) | 0.3660 | 1 | 0.3660 | 193.9 | 0.000 |
| Pressure (MPa) | 0.000400 | 1 | 0.000400 | 0.2119 | 0.652 |
| Loading × Pressure | 0.000400 | 1 | 0.000400 | 0.2119 | 0.652 |
| Error | 0.02643 | 14 | 0.001888 | | |
| SS total | 0.3933 | 17 | | | |

*Table 4. Analysis of variance for bulk density after firing.*

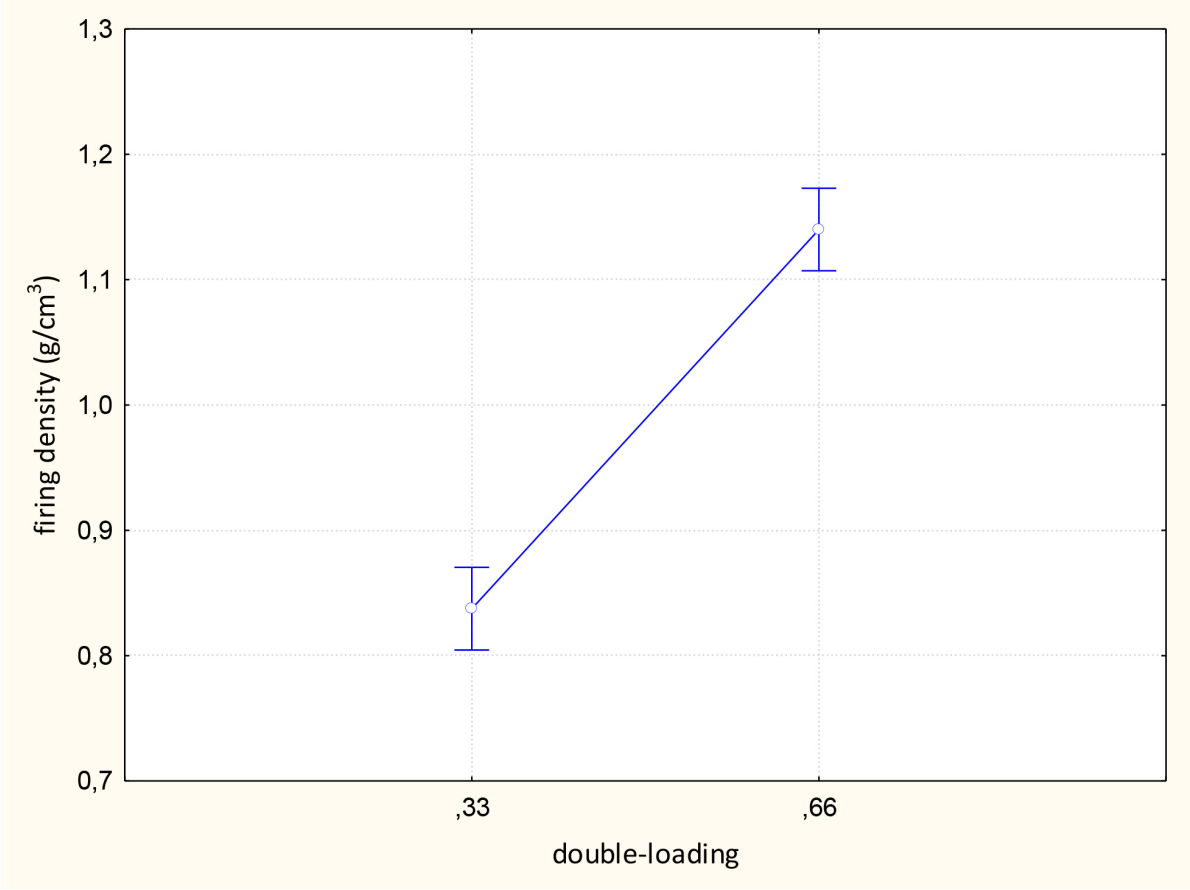


*Figure 2. Averages for the apparent density after firing as a function of double-loading.*

The graph shows the effect of the double-loading on the apparent density after firing, but in this case, the highest values of density (~1.1 g/cm$^3$) occur for double-loading with 2/3 layer of stoneware powder, which would be expected because the waste layer undergoes expansion during firing, thereby reducing the density of the final product. Therefore, the lowest density is obtained for the smallest layer of stoneware during double-loading or a larger layer of glazing waste. The lower density occurs due to expansion of the glazing waste layer during firing, since the silicon carbide undergoes oxidation from 1000°C, resulting in the formation of $SiO_2$ and $CO_2$. As this temperature is above the glass transition temperature of the glazing waste, the result is the formation of CO2 bubbles which solidify on cooling, creating the low-density cellular structure. The fit of the observed results is good ($R^2$=0.93).

Table 5 presents the analysis of variance for expansion upon firing. The variance analysis shows that, for the expansion on firing, there are two statistically significant factors: the double-loading again, with 100% reliability of the results, but also the interaction between the double-loading and pressing force, with a reliability of 97 9%. The pressing force alone had lower reliability of the results, 72.8%. The data from the analysis of variance results for expansion after firing were plotted as contour lines from a response surface, Figure 3.

| Factor | SS | dF | MS | F | p |
|---|---|---|---|---|---|
| Double-loading (%) | 77.57 | 1 | 77.57 | 394.6 | 0.000 |
| Pressure (MPa) | 0.2576 | 1 | 0.2576 | 1.310 | 0.2716 |
| Loading × Pressure | 1.328 | 1 | 1.328 | 6.757 | 0.02100 |
| Error | 2.752 | 14 | 0.1966 | | |
| SS total | 81.91 | 17 | | | |

*Table 5. Analysis of variance for the expansion after firing.*

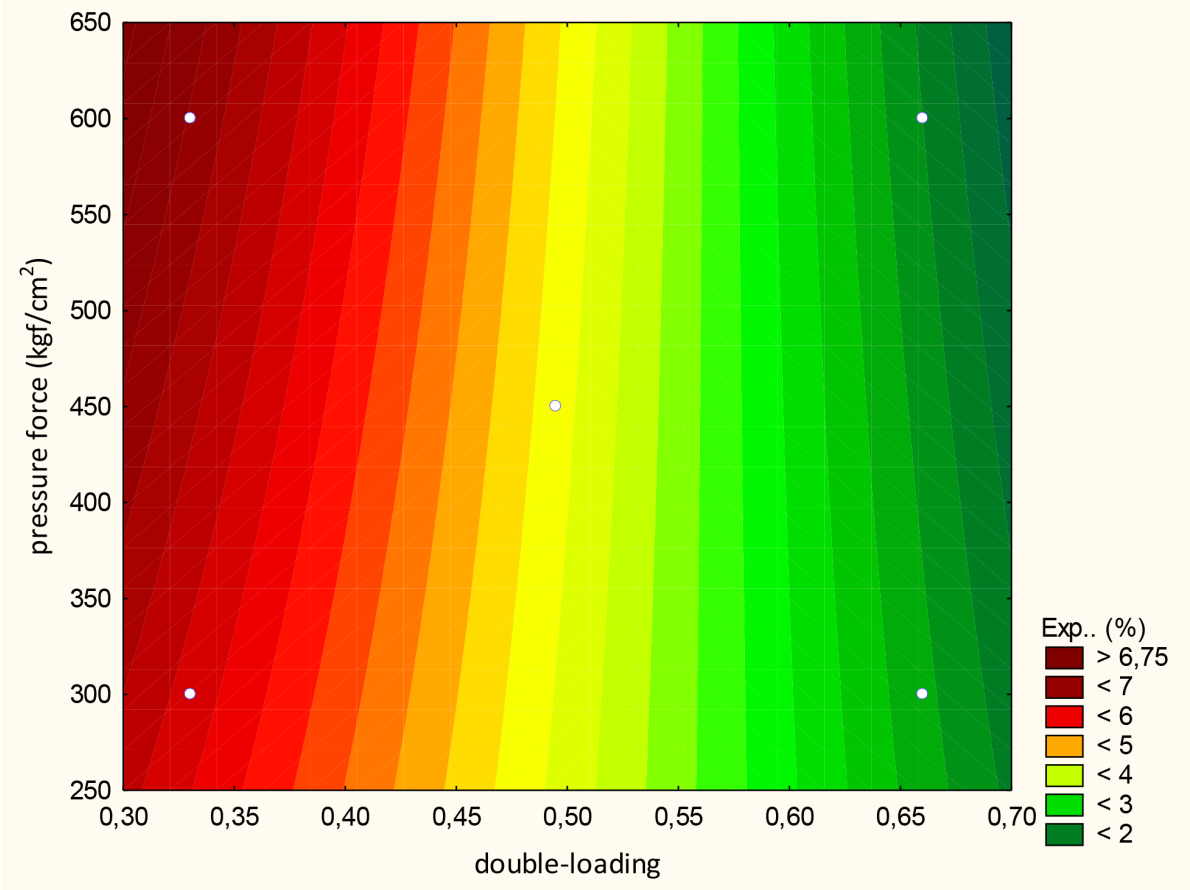


*Figure 3. Contour lines for expansion upon firing.*

The graph shows the dual effect of both the double-loading layer and the compaction force on the expansion upon firing. During double-loading, the combination of a lower layer of stoneware with a higher pressing force results in a greater expansion upon firing because of the greater amount of glazing waste that tends to expand the tile. The higher pressing force causes higher particle packing and the firing temperature causes the early formation of the impermeable glassy layer, responsible for the expansion of the tile. The fit of the observed results is good ($R^2$=0.97).

Table 6 shows the analysis of variance for water absorption. For water absorption there are two statistically significant factors: double-loading, with 99.98% reliability of the results, and the interaction between the double-loading with the pressing force, with a reliability of 97.4%. The pressing force alone was not statistically significant. The data

from the analysis of variance results for water absorption were plotted as contour lines from a response surface, Figure 4.

| Factor | SS | dF | MS | F | p |
|---|---|---|---|---|---|
| Double-loading (%) | 0.2352 | 1 | 0.2352 | 24.32 | 0.000221 |
| Pressure (MPa) | 0.000100 | 1 | 0.000100 | 0.01034 | 0.9205 |
| Loading × Pressure | 0.06003 | 1 | 0.06003 | 6.206 | 0.02591 |
| Error | 0.1354 | 14 | 0.009672 | | |
| SS total | 0.4308 | 17 | | | |

*Table 6. Analysis of variance for water absorption*

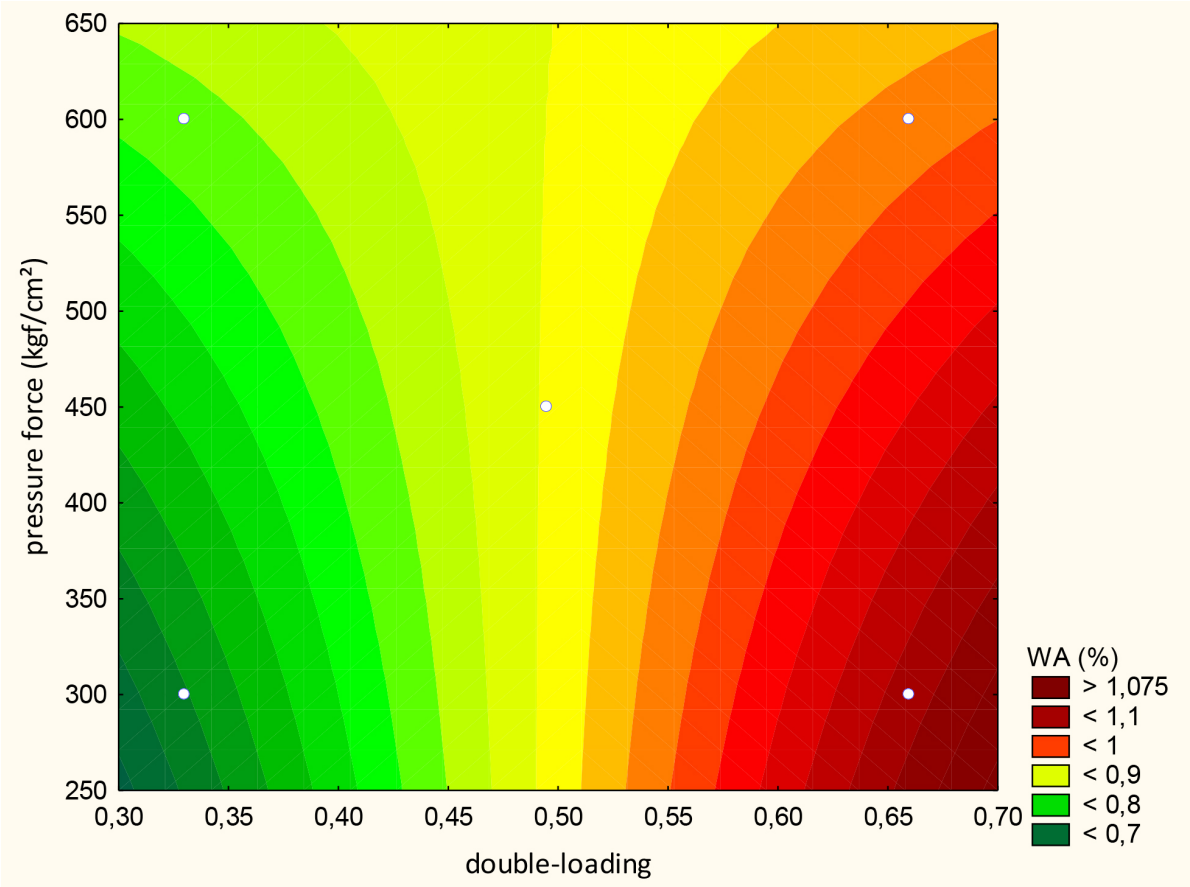


*Figure 4. Contour lines for the water absorption.*

The graph shows the dual effect of both the double-loading and the compaction force on the water absorption. The highest water absorption values (1.1%) occur for the combination of 2/3 layer of stoneware with a lower pressing force during double-loading. The stoneware substrate presents water absorption close to 2%, while the glazing waste presents no water absorption. The lowest compaction force results in a stoneware substrate presenting a more open structure after firing, thus showing greater water absorption. The fit of the observed results is not so good ($R^2$=0.69).

Finally, Table 7 shows the analysis of variance for the modulus of rupture on three-point bending. The analysis of variance shows that there are two statistically significant factors: double-loading, with ~100% reliability of the results, and the pressing force, with a reliability of 99.84%. The interaction between the double-loading and pressing force showed lower statistical significance.

| Factor | SS | dF | MS | F | p |
|---|---|---|---|---|---|
| Double-loading (%) | 175.9 | 1 | 175.9 | 40.26 | 0.000018 |
| Pressure (MPa) | 66.62 | 1 | 66.62 | 15.25 | 0.001586 |
| Loading × Pressure | 4.115 | 1 | 4.115 | 0.9420 | 0.3482 |
| Error | 61.16 | 14 | 4.369 | | |
| SS total | 307.8 | 17 | | | |

*Table 7. Analysis of variance for the modulus of rupture.*

The data from the analysis of variance results for the modulus of rupture were plotted as contour lines, Figure 5. The graph shows the effect of both the double-loading and the compaction pressure on the modulus of rupture. As expected, the highest values of modulus of rupture in bending occur for the combination of a higher pressure force with a greater layer of stoneware during double-loading because the expanded glazing waste is totally porous and thus has lower mechanical strength. Therefore, the bigger layer of stoneware substrate during double-loading, pressed at a higher compaction force, results in tiles with a higher modulus of rupture. The fit of the observed results is fair ($R^2$=0.80).

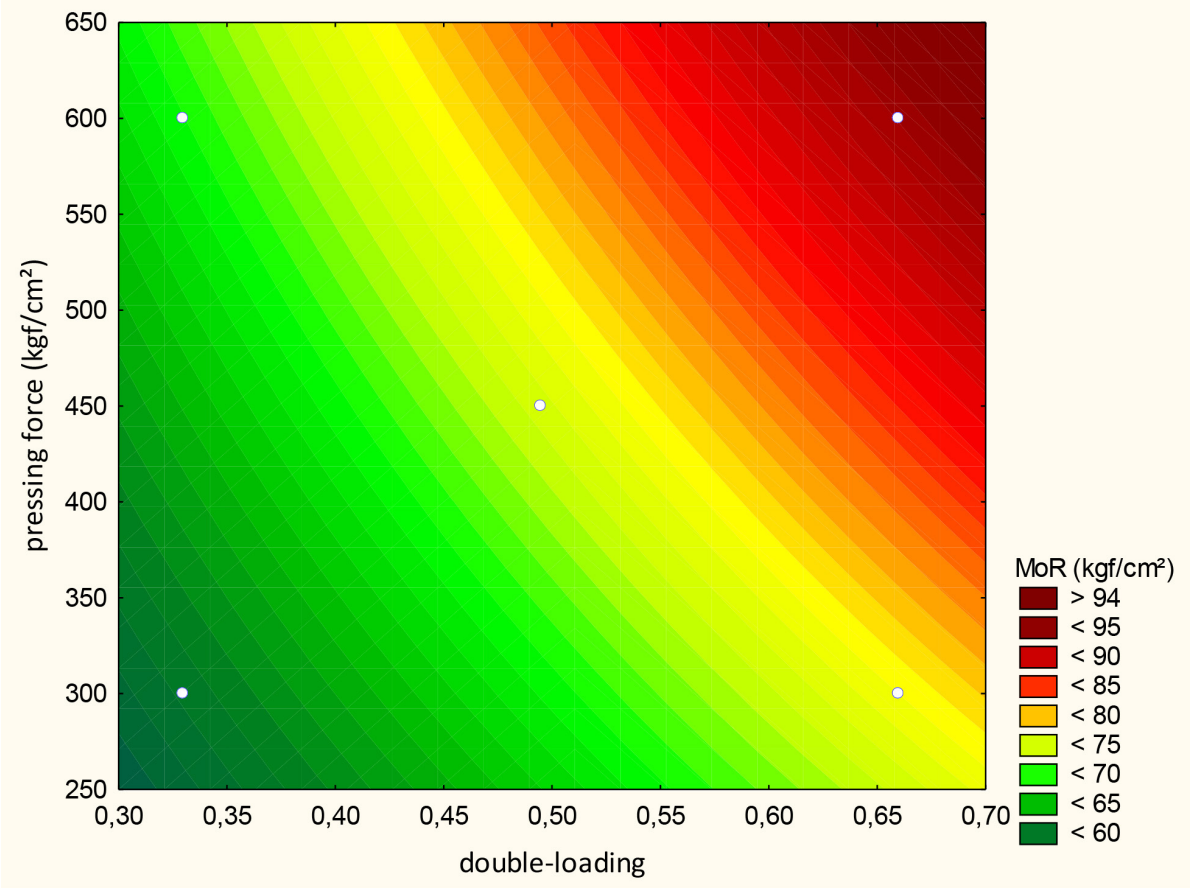


*Figure 5. Contour lines for the modulus of rupture.*

Figure 6 shows the microstructure of the sample with 33% stoneware layer (1/3) pressed at 30 MPa. Figure 6a shows the interface between the stoneware substrate (lower, solid) and Figure 6b shows the expanded glazing waste (top, porous). The micrographs clearly show the effect of SiC as a blowing agent in the glazing waste because the pores are large and rounded. All the above mentioned properties are influenced by this porous cellular structure.

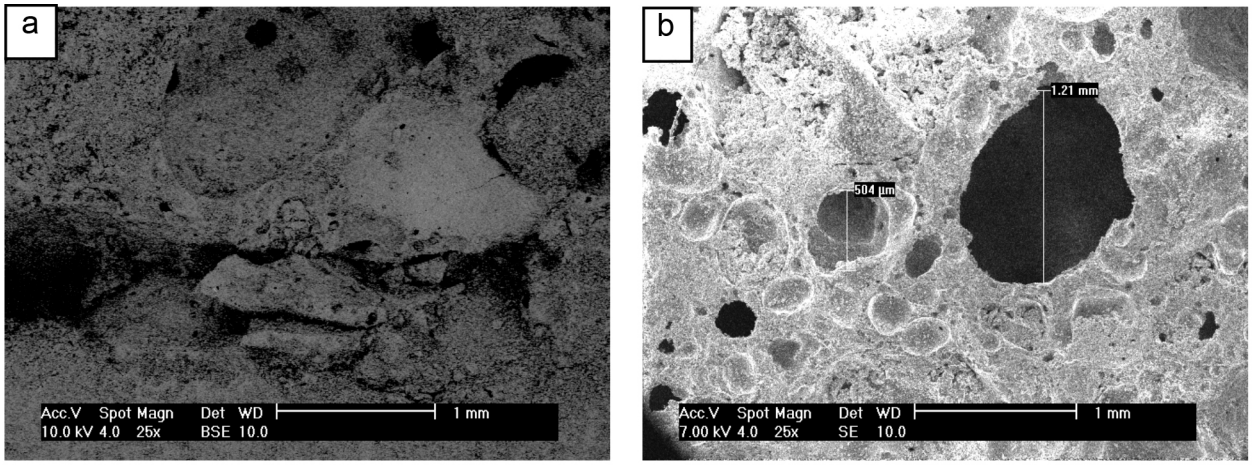


*Figure 6. Microstructure of the sample with a double load of 33% stoneware pressed at 30 MPa: a) the interface region between the stoneware substrate and the glazing waste, b) region of the glazing waste.*

## 4. CONCLUSIONS

Ceramic tiles with very low density (0.8 g/cm$^3$) were made from glazing waste. The main results were as follows:

- The bulk density of the tiles, both green and after firing, is a function solely of the double-loading during pressing. The glazing waste is responsible for the low density after firing.

- The expansion after firing depends on the interaction between the double-loading and the pressing force. The largest expansion - and thus lower density – is due to the lower amount of stoneware and higher pressing force during double-loading.

- The water absorption is also a function of the interaction between the double-loading and the pressure force, with the lowest values being obtained for the smallest fraction of stoneware pressed with lower compaction pressure, because the glazing waste does not absorb water.

- The modulus of rupture in bending depends on the double-loading layer and the pressing force. The greater moduli are obtained for the higher layers of stoneware pressed at the higher pressing forces because the porous cellular structure caused by the presence of the glazing waste decreases the resistance of the tiles.

Finally, the low density occurs due to expansion of the glazing waste during firing because silicon carbide undergoes oxidation from 1000°C, resulting in $SiO_2$ and $CO_2$, and as in this temperature the glazing waste is in the viscous state, the result is the formation of $CO_2$ bubbles which solidify on cooling, creating the cellular structure of low density.

## REFERENCES


[1] Zhang, J.-Y.; Fu, Y.-M.; Zeng, X.-M. Trans. Nonferrous Met. SOC. China 16 (2006) 453-457.

[2] Gómez de Salazar, J.M.; Barrena, M.I.; Morales, G.; Matesanz, L.; Merino, N. Materials Letters 60 (2006) 1687-1692.

[3] Richardson, J.T.; Remue, D.; Hung, J.-K. Applied Catalysis A: General 250 (2003) 319-329.

[4] Atwood, R.C.; Jones, J.R.; Lee, P.D.; Hench, L.L. Scripta Materialia 51 (2004) 1029-1033.

[5] Kishimoto, A.; Obata, M.; Asaoka, H.; Hayashi, H. Journal of the European Ceramic Society 27 (2007) 41-45.

[6] Rul, S.; Laurent, Ch.; Peigney, A.; Rousset, A. Journal of the European Ceramic Society 23 (2003) 1233-1241.

[7] Costa Oliveira, F.A.; Dias, S.; Fátima Vaz, M.; Cruz Fernandes, J. Journal of the European Ceramic Society 26 (2006) 179-186.

[8] Maire, E.; Colombo, P.; Adrien, J.; Babout, L.; Biasetto, L. Journal of the European Ceramic Society 27 (2007) 1973-1981.

[9] Zhang, Y. Materials Research Bulletin 39 (2004) 755-761.

[10] Sharafat, S.; Ghoniem, N.; Sawan, M.; Ying, A.; Williams, B. Fusion Engineering and Design 81 (2006) 455-460.

[11] Bernardin, A.M.; Felisberto, D.S.; Daros, M.T.; Riella, H.G. Cerâmica Industrial 11 (2006) 31-34.

[12] Bernardin, A.M.; Silva, M.J.; Riella, H.G. Materials Science & Engineering A 437 (2006) 222-225.

[13] Pereira, A.S.; Felisberto, D.S.; Daros, M.S.; Luckmann, G.; Bernardin, A.M. En: X Congreso Mundial de la Calidad del Azulejo y del Pavimento Cerámico. Castellón: Cámara Oficial de Comercio, Industria y Navegación (2008) 3:83-87.

[14] Marques, A.M.; Bernardin, A.M. En: X Congreso Mundial de la Calidad del Azulejo y del Pavimento Cerámico. Castellón: Cámara Oficial de Comercio, Industria y Navegación (2008) 3: 89-93.

[15] Bernardin, A.M.; Silva, M.J.; Silva, H.G.C.; Riella, H.G. En: IX Congreso Mundial de la Calidad del Azulejo y del Pavimento Cerámico. Castellón: Cámara Oficial de Comercio, Industria y Navegación (2006) 3: 189-196.